

## Interaction of Water with Titania: Implications for High-Temperature Gas Sensing

Joseph Trimboli,<sup>†</sup> Matthew Mottern,<sup>‡</sup> Henk Verweij,<sup>‡</sup> and Prabir K. Dutta<sup>\*,†</sup>

Department of Chemistry, The Ohio State University, 100 East 18th Avenue, Columbus, Ohio 43210-1185, and Department of Materials Science and Engineering, The Ohio State University, 477 Watts Hall, 2041 College Road, Columbus, Ohio 43210

Received: September 12, 2005; In Final Form: January 26, 2006

High-temperature gas sensors based on semiconducting metal oxides show potential for optimization of combustion processes, resulting in efficient energy use and minimization of emissions. Such metal oxides can function as gas sensors because of the reaction of the sensing gas (e.g., CO) with ionosorbed oxygen species on the oxide surface with the resulting increase in conductivity. A limitation of metal oxide sensors is their difficulty of distinguishing between different gases. Designing selectivity into sensors necessitates a better understanding of the chemistry of gas–solid interactions at high temperatures. In this paper, we have used in situ infrared spectroscopy to monitor the dehydration of a hydrated anatase surface up to 600 °C and also to examine the hydration/dehydration of anatase held at 400 °C. When the O–H stretching region (3000–3800 cm<sup>-1</sup>) was primarily focused on, it was found that water loss from the titania surface proceeded at lower temperatures (<200 °C) through desorption, whereas at higher temperatures, water dissociation to terminal (~3710 cm<sup>-1</sup>) and bridged (~3660 cm<sup>-1</sup>) hydroxyl groups was noted. With a further increase in temperature to 600 °C, the bridged hydroxyl groups disappeared faster than the terminal ones. The electrical resistance of anatase at 600 °C was measured in the presence of moist gas streams and resulted in an increase in conductivity in the presence of water. In situ vibrational spectroscopy indicated a temporal correlation between the appearance of the bridging hydroxyl group and the change in electrical resistance. Several possible mechanisms are discussed. The chemical reaction of water with anatase at high temperatures necessitates that water be removed from the gas stream to avoid interference. A strategy involving the use of a hydrophobic microporous filter that can reject water and let gases such as CO pass unimpeded is examined. Successful use of such a concept has been demonstrated with a silicalite filter using moist CO gas streams.

### Introduction

The alteration of the surface properties of titania by reaction with water at high temperatures are important in catalysis<sup>1</sup> and sensing.<sup>2,3</sup> For sensing applications, the change in resistance of semiconducting metal oxides such as tin oxide and titania upon exposure to gases is the basis for their use as sensors. In developing sensors, one of the critical elements is minimizing interferences. It has been noted that metal oxides show a change in resistance when water is introduced in the presence of gases such as CH<sub>4</sub> and CO.<sup>2,3</sup> Understanding the cross sensitivity of metal oxide devices toward moisture is necessary, and fundamental studies have been conducted to examine the way in which water changes the resistance of metal oxide surfaces.<sup>4–6</sup> Infrared spectroscopy has been the method of choice to study the interaction of water with titania,<sup>7–12</sup> and the role of hydroxyl groups in modifying surface properties has been proposed. Heiland and Kohl, for example, have suggested that the hydroxyl groups formed on the surface will ionize and can cause electrons to be injected into the conduction band of the titania.<sup>4</sup> Combination of infrared emission measurements with conductivity between 250 and 650 °C has been reported for Ga<sub>2</sub>O<sub>3</sub>, and it was concluded that hydroxyl groups can lead to either increased or decreased conduction depending on the electron-transfer

reactions.<sup>6</sup> We have exploited the resistance change in anatase due to water for designing a sensor for detecting propane in the presence of CO.<sup>13</sup> In the presence of a catalyst (Pt–zeolite Y) both CO and propane are oxidized, with the CO forming CO<sub>2</sub>, which does not alter the resistance of the anatase, whereas propane releases water during combustion that causes a resistance change.<sup>13</sup>

In the present study, we have focused on correlating the changes in resistance of anatase in the presence of water using in situ diffuse reflectance infrared spectroscopy at temperatures up to 600 °C, mimicking conditions similar to those present during resistance measurements. By correlating the resistance changes with the spectroscopic data, possible models that explain how the presence of moisture alters the resistance of anatase are proposed. Since the spectroscopic studies suggest that the effect of water can only be minimized by keeping water from reaching the semiconducting surface, we have examined the use of hydrophobic zeolite filters for the rejection of water. The efficiency of the filter in rejecting water is monitored by measuring resistance changes of anatase films at 600 °C in the presence of moist gas streams.

### Experimental Section

**Materials Preparation.** *Anatase.* To prepare films for resistance measurements, commercial anatase (Aldrich, 99.9%+ purity) was milled using zirconia balls in 2-propanol for 4 h.<sup>14</sup> The resultant powder was heated at 800 °C for 6 h, combined with a binder (V-801 Heraeus), a solvent (5V-507 Heraeus),

\* Author to whom correspondence should be addressed. E-mail: dutta.1@osu.edu.

<sup>†</sup> Department of Chemistry.

<sup>‡</sup> Department of Materials Science and Engineering.

and dispersant (BYK Chemie), and sonicated for an hour (Branson 2210 sonicator). This paste was then screen-printed onto a 1.5 cm<sup>2</sup> alumina substrate that had gold interdigitated electrodes and heated at 200 °C for 2 h and then at 800 °C for 6 h. Powder diffraction showed that the anatase phase is maintained after sample preparation.

Two anatase samples were prepared for X-ray photoelectron spectroscopy (XPS). The first powder was heat-treated at 800 °C as described above and stored under ambient conditions. The second sample after heating was exposed to wet air at room temperature for 15 min, evacuated overnight, heated to 600 °C in a slight vacuum ( $\sim 1 \times 10^{-2}$  Torr), and transferred in a nitrogen environment into the XPS sample chamber.

For infrared spectroscopy, anatase was milled for 4 h in 2-propanol and calcined at 800 °C for 6 h, and the process was repeated twice to mimic the thermal conditions used for electrical measurements.

**Silicalite/Alumina Filter.** Silicalite was synthesized on a porous alumina disk. The alumina disk was prepared by combining 1.6 g of alumina (Baikowski International Corporation, BaikaloX CR 10) with a few milliliters of water and ground with a mortar and pestle. Pellets were pressed using a 0.75 in. i.d. steel die and  $\sim 11\,000$  pounds of pressure for 2 min. Once pressed, the disks were left to dry at 40 °C in an oven for 3 days. The disks were then heated to 1200 °C with a ramp rate of 2 °C/min and allowed to dwell at this temperature for 5 h. The cooling rate was 5 °C/min. When complete, all disks were polished with 320 grit sandpaper. The synthesis of silicalite on the alumina was done by literature procedures.<sup>15,16</sup> Silicalite was made by adding 0.85 g of NaOH to 60 mL of 1.0M TPAOH (Aldrich) and stirring until the NaOH dissolved. Fifteen grams of fumed silica was added to the liquid. The gel was then heated to 80 °C, placed in Teflon cups in a Parr bomb, and heated to 125 °C for 8 h.

The solid was recovered by centrifugation, dried, and examined by powder diffraction to confirm the silicalite phase. The seed solution for membrane growth was prepared by adding 0.075 g of the silicalite to 15 mL of a NH<sub>4</sub>OH solution (pH 9). The alumina membrane was dipped into the seed solution for  $\sim 30$  s and dried, and the process was repeated twice.

The seeded alumina was placed in a solution with a molar ratio of 3:25:1500 (TPAOH/SiO<sub>2</sub>/H<sub>2</sub>O) at an angle with a small piece of glass, with the seed side facing downward. The Teflon cup was sealed inside a Parr bomb and placed inside an oven preheated to 175 °C for 24 h. The recovered disks were washed several times with hot water, dried, and then heated from room temperature at a ramp of 0.2 °C/min to 350 °C with a dwell of 6 h. From that point they were heated at a ramp of 0.2 °C/min to 525 °C with a dwell of 5 h. Finally the disks were cooled at a rate of 0.5 °C/min to room temperature.

**Materials Characterization.** Powder diffraction data were taken with a Rigaku Geigerflex X-ray powder diffractometer using Cu K $\alpha$  radiation, and scanning electron microscopy (SEM) was performed with a XL-30 E SEM FEG instrument.

X-ray photoelectron spectroscopy studies were performed with a Kratos AXIS Ultra X-ray photoelectron spectrometer. An Al source was used for all measurements. The binding energies were calibrated with the C 1s peak at 284.8 eV. Experiments were done at a resolution of 0.1 eV with a pass energy of 20 eV.

Humidity measurements were obtained with a sensor manufactured by Vaisala (DMP dewpoint transmitter model 248), which was placed directly into the gas stream via Swagelok pipes and fittings.

Diffuse reflectance infrared Fourier transform spectroscopy (DRIFTS) was performed with a Bruker IFS 66/S spectrometer equipped with a high-temperature/high-pressure chamber from Spectra-Tech. This chamber could be heated to temperatures of up to 750 °C during infrared studies with controlled concentrations of gases. ZnSe windows were employed in the dome of the chamber because they are resistant to water degradation. A mercury cadmium telluride (MCT) detector was used, and a gas flow of 30 cm<sup>3</sup>/min was established for all tests.

Two sets of DRIFTS experiments were performed. The first involved heating the anatase powder to 750 °C in dry flowing air for a minimum of 30 min to remove as much adsorbed water as possible. The powder was then cooled to room temperature, hydrated with 16 000 ppm of water, and heated at 100 °C increments up to 600 °C, dwelling for 10 min at each step to obtain spectra.

The second set of experiments involved heating anatase to 750 °C for a minimum of 30 min. After this was completed, the powder was cooled to 400 °C and exposed  $\sim 16\,000$  ppm water, with spectra being recorded immediately. The spectra were also recorded at 400 °C after the flow of water was stopped.

It was observed that beyond  $\sim 350$  °C the signal received by the MCT detector decreased dramatically, which required continual alignment to attain a signal at higher temperatures. Shreedhara et al. noted similar issues and attributed the behavior to thermal expansion of the sample container as their material was heated.<sup>17</sup> In our experiments a visible change in sample position could be noted during the heating process that caused the titania to rise up from the sample cup. Carefully aligning the cell as this phenomenon was occurring was necessary.

A spectrum of dry titania taken at 750 °C was used as the reference for the Kubelka–Munk transformation. The choice of this sample was based on the fact that scattering from this sample would be optimum without any complications from any absorbing peaks. The spectrum at 750 °C was multiplied by a positive constant to increase the position of that spectrum on the y-axis (reflectance).<sup>18</sup>

**Electrical Measurements.** To conduct resistance measurements, the anatase film was placed in a quartz cylinder housed within a tube furnace and attached via gold leads to either a 34401A HP multimeter or a 34970A HP multiplexer.<sup>14</sup> The flow of gases used was determined with digital mass flow controllers manufactured by Sierra.<sup>14</sup> Water was added by passing gas over a small glass boat filled with water. The silicalite/alumina disks used were  $\sim 2$ -mm-thick and were sealed inside a stainless steel housing with two ports on each side of the device to allow gas to be applied against the membrane and contained O-rings to maintain a gastight seal around the membrane. Gases passing through this device were then directed on to the anatase film for resistance measurements.

## Results

**Studies with Anatase. Resistance Changes of Anatase with Gases.** The anatase films were heated to 600 °C in flowing 5% O<sub>2</sub>/N<sub>2</sub> to establish a baseline resistance ( $R_0$ ). Once stabilized, baseline drifts were  $< 2\%$  over a 10 min period. To generate water vapor, 5% O<sub>2</sub>/N<sub>2</sub> was passed over a small quartz boat filled with water, and this stream was passed over the anatase film. With a humidity sensor, it was determined that the gas stream contained  $\sim 16\,000$  ppm of water. The resistance change upon introduction of water is shown in Figure 1a, stabilizing at a value of  $R$  within 3 min, with the overall change in resistance represented by  $R/R_0$  of 0.80. When dry 5% O<sub>2</sub>/N<sub>2</sub> was passed,

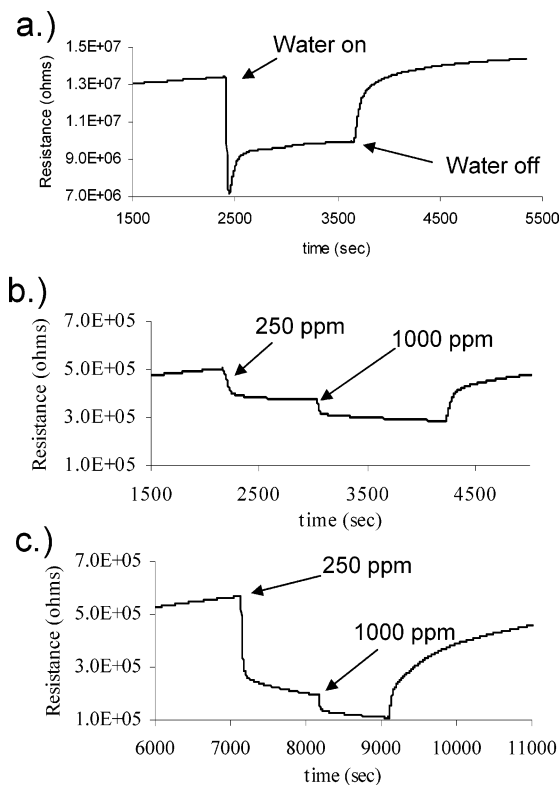


**Figure 1.** Change in electrical resistance of anatase films at 600 °C to (a) 16 000 ppm water, (b) 250, 1000 ppm of propane, and (c) 250, 1000 ppm of CO (background gas is 5% O<sub>2</sub>/N<sub>2</sub>).

the resistance recovered to the baseline within 15 min. Figure 1b shows data on a different anatase films with 250 and 1000 ppm propane;  $R/R_0$  values were 0.75 and 0.55, respectively, and with 250 and 1000 ppm CO,  $R/R_0$  values of 0.33 and 0.23, respectively were observed, all at a temperature of 600 °C. The background resistances vary between different film preparations and is the reason that comparison is made based on  $R/R_0$ .

**X-ray Photoelectron Spectroscopy.** XPS analysis on anatase focused on two samples. The first was heat-treated anatase (800 °C for 6 h) stored under ambient conditions. The second sample was prepared by hydrating preheated anatase at room temperature and then heating at 600 °C to dehydrate the sample, and transferred to the XPS sample chamber under anaerobic conditions. Figure 2 shows the XPS data in the O 1s region. For the ambient exposed sample, the spectrum was deconvoluted into three peaks, a peak centered at binding energy 532.2 eV (relative area of 34.7%), a peak centered at 530.7 eV (relative area of 28.5%), and a third peak centered at 529.9 eV (relative area of 36.8%), shown in Figure 2a. The dehydrated anatase sample shown in Figure 2b exhibited two peaks at 530.9 eV (relative area of 31.6%) and 529.9 eV (relative area 68.4%).

**Infrared Studies of the Dehydration of Anatase.** Spectra were obtained in situ as a hydrated anatase sample was heated from room temperature to 600 °C. All spectra were acquired using a Kubelka–Munk transformation with a spectrum of anatase at 750 °C as the reference. Figures 3 and 4 show the spectra obtained at different temperatures. At 25 °C, bands are observed at 1645 cm<sup>-1</sup>, a broad band at 3300 cm<sup>-1</sup>, and a sharp peak at 3697 cm<sup>-1</sup>. As the temperature is increased to 100 °C, the bands at ~3300 and 1645 cm<sup>-1</sup> are reduced in intensity (Figure 3a).

When the temperature is increased to 200 °C (Figure 3b), the spectrum is dominated by a band at ~3190 cm<sup>-1</sup> (shoulder at ~3450 cm<sup>-1</sup>), which is present up to temperatures of 600

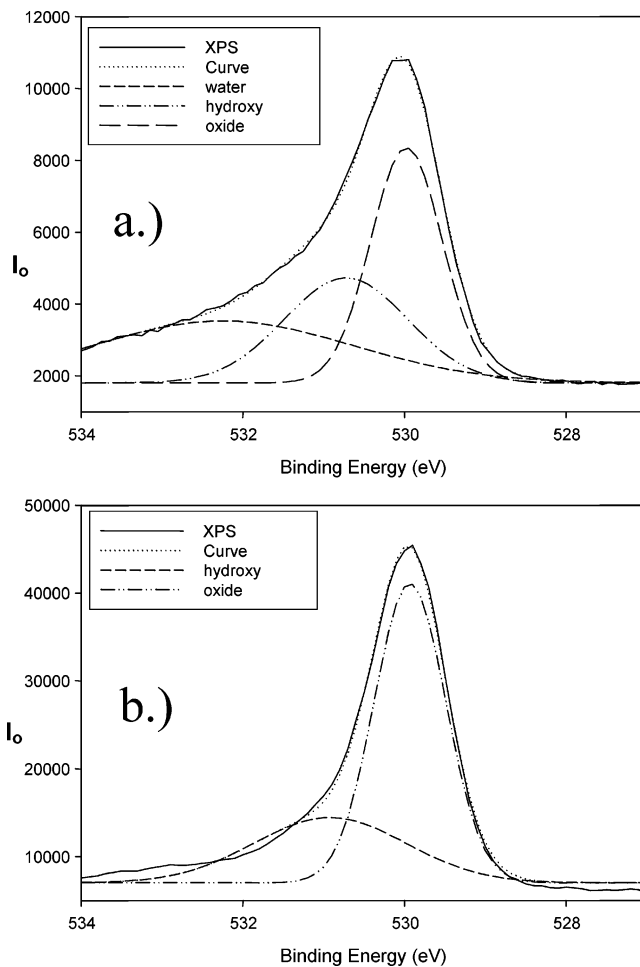


**Figure 2.** XPS data for the O 1s region of anatase: (a) ambient exposed sample and (b) dehydrated sample.

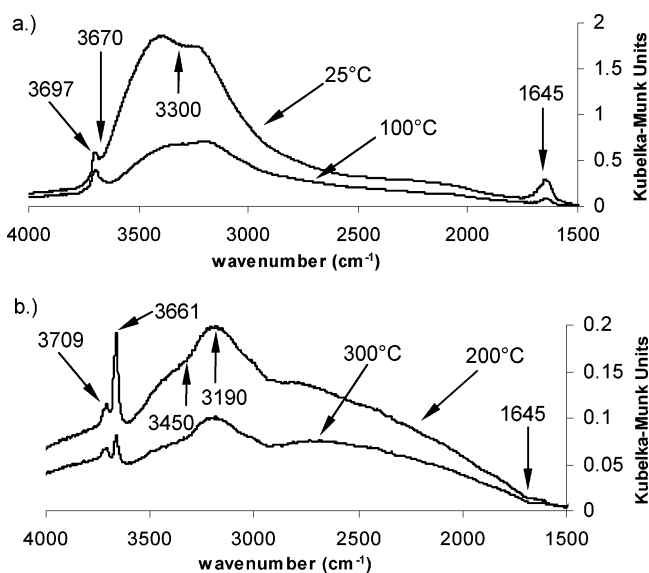


**Figure 3.** Infrared spectra of a hydrated sample of anatase at different temperatures: (a) 25 and 100 °C and (b) 200 and 300 °C.

°C. Also, the peak at 1645 cm<sup>-1</sup> has disappeared at this temperature. In addition, two new sharp peaks, one located at 3709 cm<sup>-1</sup> and the other at 3661 cm<sup>-1</sup>, are observed. Increasing the temperature to 300 °C shows a decrease of the peak at 3661 cm<sup>-1</sup> compared to the peak at 3709 cm<sup>-1</sup>. This trend continued

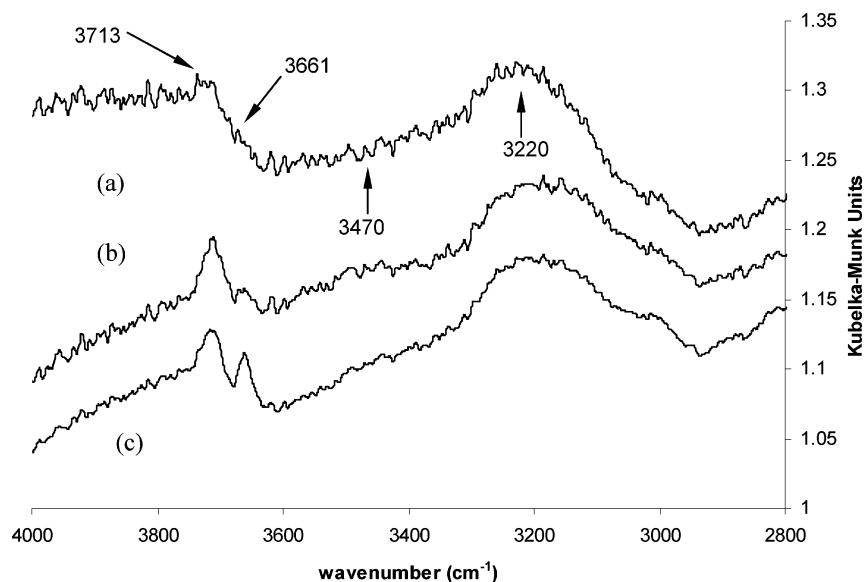


**Figure 4.** Infrared spectra of hydrated anatase at: (a) 600, (b) 500, and (c) 400 °C.

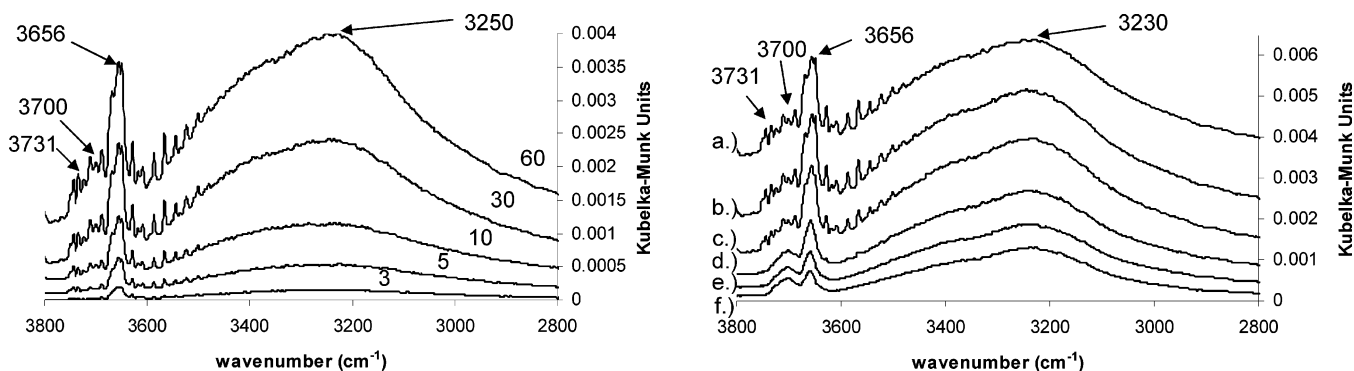


**Figure 5.** Infrared spectra of dehydrated anatase at 400 °C as a function of time upon exposure to 16 000 ppm water. Spectra are taken after 3, 5, 10, 30, and 60 min of hydration. Spectra ascend with increasing hydration times.

with temperature as shown for 400–600 °C in Figure 4. As the temperature approached 600 °C, the 3661  $\text{cm}^{-1}$  has disappeared, and the peak at 3713  $\text{cm}^{-1}$  is weak.

**Infrared Studies of Exposure of Anatase to Water at High Temperatures.** The anatase was held at 400 °C in an atmosphere of 5%  $\text{O}_2/\text{N}_2$ ,  $\sim 16\,000$  ppm water was introduced, and spectra were recorded in situ as a function of time. As shown in Figure 5, several spectroscopic changes are evident within the first 3 min. A sharp band at 3656  $\text{cm}^{-1}$  and a weak broad band at  $\sim 3250$   $\text{cm}^{-1}$  are observed. With time, these bands grow, along with appearance of bands at 3700 and 3731  $\text{cm}^{-1}$ . When the flow of water was stopped and replaced with a dry background gas, the peaks at  $\sim 3230$   $\text{cm}^{-1}$  and the sharp peaks at 3656, 3700, and 3731  $\text{cm}^{-1}$  all begin to decrease, as shown in Figure 6. However, the peak at 3656  $\text{cm}^{-1}$  undergoes the most significant decrease relative to the other peaks. After 50 min of dehydration, this peak is actually less intense than the peak at 3700  $\text{cm}^{-1}$ .

**Studies with Zeolite Filter: Role of a Zeolite Filter To Minimize Water Transport.** A strategy to minimize the effect of water on resistance of titania is to exclude the water from the solid. One of the ways to do this is to use a hydrophobic microporous membrane that rejects water but can let other gases pass through. We tested this concept by examining a silicalite film synthesized on an alumina support to form a filter. Silicalite

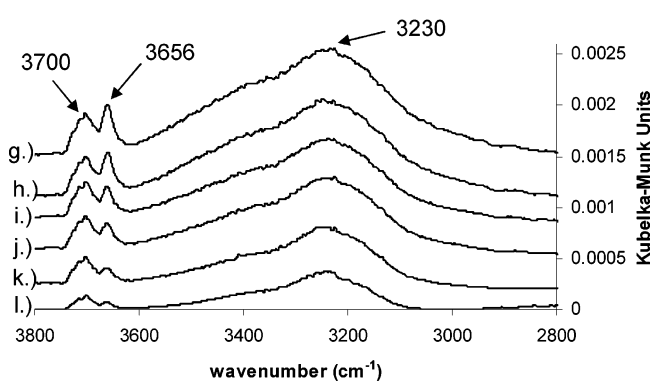


**Figure 6.** Infrared spectra of anatase at 400 °C as dehydration is occurring over a 101 min period. A spectrum after 60 min of constant water exposure (labeled “a” in the graph) prior to the dehydration process is provided for reference. Other spectra shown are taken after the flow of water was stopped after: (b) 15, (c) 17, (d) 18, (e) 20, (f) 25, (g) 30, (h) 35, (i) 50, (j) 60, (k) 91, and (l) 101 min.

with two channels of  $0.54 \times 0.56 \text{ nm}^2$  and  $0.51 \times 0.55 \text{ nm}^2$  is suitable for this purpose, and the synthesis of silicalite membranes is well established.<sup>15,16</sup>

The diffraction pattern for the seeded membrane had peaks characteristic of silicalite as well as the alumina support (data not shown). Scanning electron microscopy of the zeolite/alumina membrane shown in Figure 7 indicates a surface consisting of intergrown zeolite crystals with a film thickness of  $\sim 10 \mu\text{m}$ .

The silicalite/alumina filter was placed in a stainless steel housing positioned before the oven containing the anatase film.

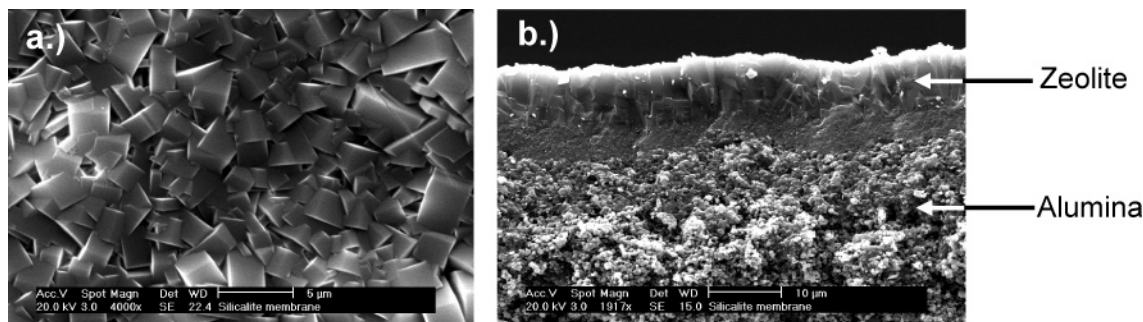


**Figure 7.** SEM of silicalite membrane on alumina support shown from a (a) top-down view and (b) a cross-sectional view.

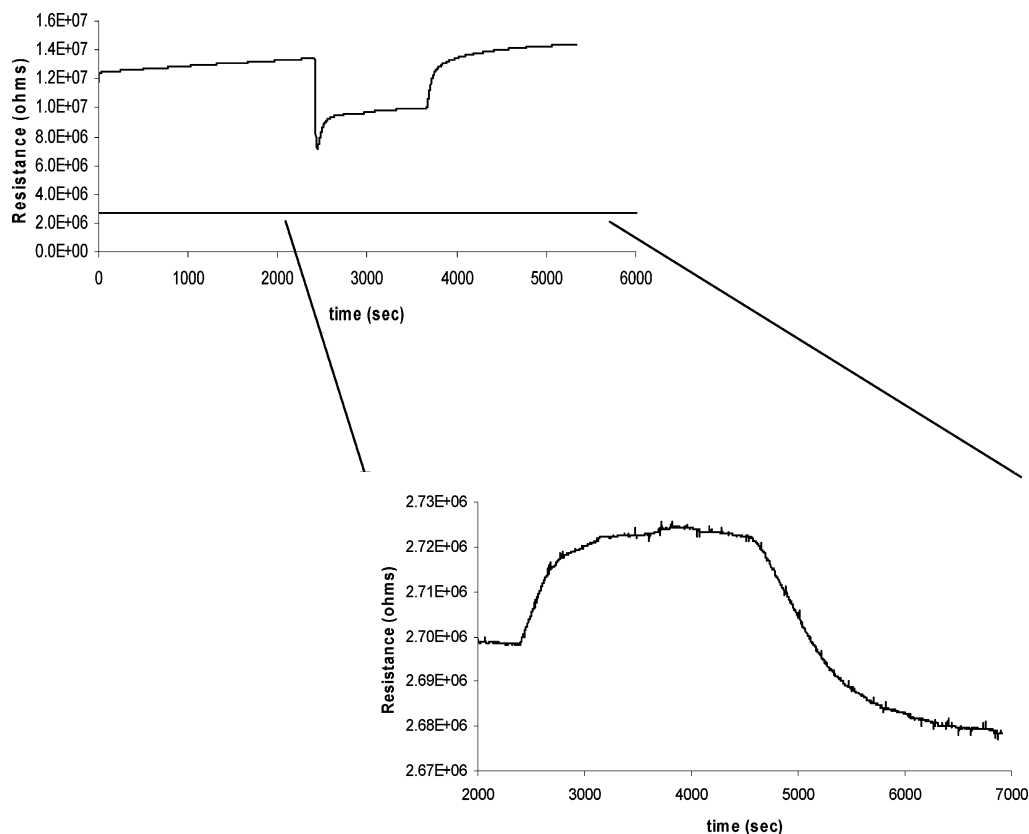


**Figure 8.** Resistance change of anatase film at 600 °C as the gas stream is changed from (a) dry air to wet air (16 000 ppm water) and (b) for a second anatase film as gas stream is changed from dry air to wet air (16 000 ppm) but passing through the silicalite filter before going over the anatase film. (A magnification of the resistance is shown in curve b.)

A baseline resistance of anatase was established at 600 °C in flowing air ( $R_0 = 2.70 \times 10^6 \text{ M}\Omega$ ), and then a hydrated air stream ( $\sim 16\,000$  ppm water) was passed through the silicalite filter and onto the anatase film. The resistance rose very slightly due to this change ( $R/R_0 = 1.01$ ) and is not even evident in Figure 8b (see insert for magnified y-scale); the reason for this slight increase is unclear. When the gas composition was changed back to dry air, the resistance of the sensor recovered. Figure 8a shows the same data as Figure 1a and is the resistance change that occurs if the moist stream is directly exposed to an anatase film.

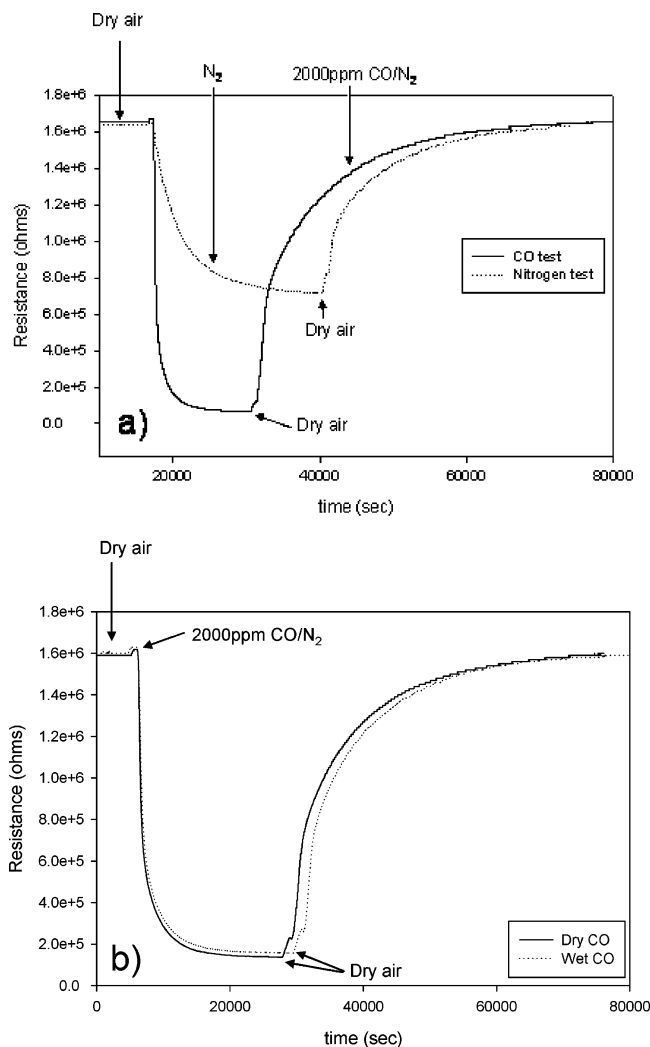
In another test using the silicalite membrane, after the baseline was established at 600 °C, nitrogen was introduced, and the resistance decreased ( $R/R_0 = 0.5$ ), as shown in Figure 9a. This experiment was repeated with 2000 ppm CO in a balance of nitrogen and leads to a significantly greater reduction in resistance ( $R/R_0 = 0.15$ ) via the added reaction of CO with titania (Figure 9a).

Figure 9b shows the data using humid CO. The introduction of 2000 ppm of wet CO passing through the silicalite membrane gave the same response as dry CO, indicating that the membrane is effective in removing the interference by water.

## Discussion

Resistance changes observed in anatase in the presence of propane and CO as shown in Figures 1b and 1c occur because of reaction of the gas with ionosorbed oxygen species, resulting in lowering of the barrier toward electron transport between grains, which is the accepted reaction mechanism for metal oxides (e.g.,  $\text{SnO}_2$ ).<sup>5</sup> With water, the decrease in resistance must arise from a different mechanism since redox chemistry of water is unlikely.

X-ray photoelectron spectroscopy peaks due to O 1s in anatase are reported at 529.9 eV for lattice oxygens, OH groups at 531.5 eV, and molecular  $\text{H}_2\text{O}$  at 532.8 eV.<sup>19</sup> The ambient



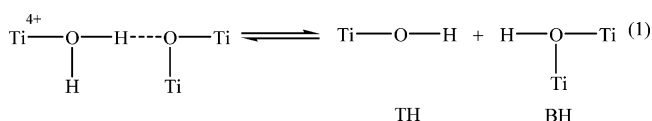
**Figure 9.** (a) Change in the resistance of an anatase film at 600 °C upon passing 2000 ppm CO (in nitrogen) and nitrogen alone. (b) Change in the resistance of an anatase film at 600 °C upon passing 2000 ppm CO (in nitrogen) in both dry and wet environments. Background resistance in all cases measured in dry air, and all gases pass through the silicalite membrane prior to exposure to anatase.

exposed anatase sample exhibited a broad peak centered around 532.2 eV (Figure 2) corresponding to molecular water, whereas with dehydrated anatase (600 °C), there was a contribution only from surface hydroxyl groups at 530.9 eV, confirming that high-temperature treatment leads to loss of adsorbed water, but hydroxyl groups are still present on the surface.

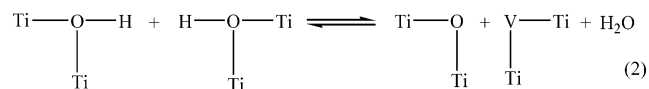
There have been a large number of infrared spectroscopic studies of water on anatase.<sup>7–12</sup> Our contribution in this paper has been to do in situ spectroscopic studies of dehydration up to 600 °C and also in situ studies of the effect of water uptake and loss at 400 °C, with the goal of correlating resistance changes measured at high temperatures with surface species. The spectroscopic assignments we discuss below are based on previous studies.<sup>7–12</sup>

As expected, upon being heated to 200 °C, the molecular water is removed as shown by the decrease of the 1645, 3300, and 3697 cm<sup>-1</sup> peaks (Figure 3). Two new bands at 3709 and 3661 cm<sup>-1</sup> formed at 200 °C have been assigned to terminal (TH) and bridging hydroxyl (BH) groups, respectively. On the basis of the literature, the most plausible model for adsorbed water dissociation involves the following steps.<sup>10,20</sup> The water molecule is coordinated to a five-coordinated Ti<sup>4+</sup> and in

addition can form a hydrogen bond with neighboring bridging oxygen atoms. The hydrogen bonding can promote the dissociation, as shown in reaction 1.



The dissociation of H<sub>2</sub>O as outlined in reaction 1 should lead to TH and BH groups and is observed beginning at 200 °C (Figure 3). The assignment of the band at ~3200 cm<sup>-1</sup> observed at temperatures exceeding 300 °C is not clear. Earlier studies have noted bands at ~3400 cm<sup>-1</sup> even after evacuation at 400 °C. Bands in this region cannot be due to hydrogen-bonded water molecules, since these would have been lost at much lower temperatures. Possibilities include strongly chemisorbed water at isolated sites.<sup>11</sup> When the temperature increases (Figures 3 and 4), there is a decrease in intensity of the bands due to TH, BH, and chemisorbed water due to loss of water from the surface. The band at ~3710 cm<sup>-1</sup> due to TH groups, though decreased, survives up to 600 °C (Figure 4) as compared to the band at ~3660 cm<sup>-1</sup> due to BH groups. The initial loss of the bridging OH groups over the terminal groups upon dehydroxylation has been noted by a Primet et al.<sup>21</sup> In addition to the reverse of reaction 1, nests of BH groups can exist, which can undergo H<sub>2</sub>O loss as outlined in reaction 2



where V represents an oxygen vacancy.

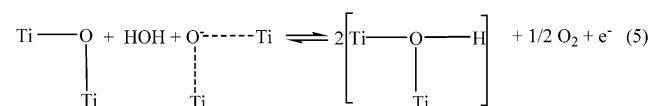
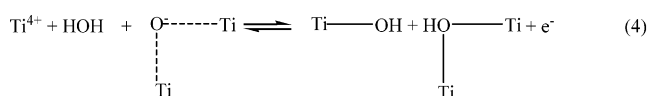
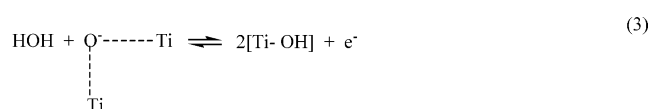
#### Correlation of Surface Analysis to Resistance Changes.

Upon introduction of water at 400 °C, the band due to BH groups is the primary band within the first 3 min, and with time, the emergence of the 3250 cm<sup>-1</sup> band as well as the 3700 cm<sup>-1</sup> bands is clear (Figure 5). The process shown in reaction 1 leading to TH and BH groups is clearly occurring over a ~60 min period (Figure 5). During the first 15 min after the supply of water vapor is stopped, the BH group is also the one to lose intensity (Figure 6). It is also noted in the present study that during measurement of change in resistance the steady-state response to water occurs within ~3 min of exposure (Figure 1a). This means that all of the electrically important events, i.e., those actions which give rise to a resistance change, have all happened within 3 min. Also, the resistance is stable during long-term water exposure; it shows no additional drift. As the water is turned off, the resistance change reaches steady state within 15 min (Figure 1a). This means that any additional species that form or are removed from the titania surface after 15 min have no effect on the resistance of the sensor.

There are several models in the literature attempting to explain the changes in resistance of metal oxide semiconductors at elevated temperatures upon exposure to water. Heiland and Kohl propose that for tin oxide exposed to water hydroxyl groups bind to tin with the protons attaching to lattice oxygen and charge injection into the oxide.<sup>4</sup> Pohle et al. who studied Ga<sub>2</sub>O<sub>3</sub> sensors provided an alternative model.<sup>6</sup> This group concluded from infrared emission studies that several reactions due to the presence of water occur, and some of them can lead to increased conductance while others boost the resistance instead. Ionization of adsorbed water resulting in electron injection as well as formation of hydroxyl groups bound to gallium and lattice oxygen has been proposed.

Henrich and Cox suggest that when water molecules are chemisorbed it leads to removal of surface oxygen.<sup>22</sup> Though the idea that adsorbed water provides a barrier to ionosorption of oxygen has been discussed, there is no information on the nature of the adsorbed site.<sup>2</sup>

It has been suggested that surface ionosorbed oxygen on tin oxide changes from  $O_2^-$  to  $O^-$  to  $O^{2-}$  as the temperature increases.<sup>9,23</sup> For  $O_2$  chemisorption on titania, low-temperature studies have shown the presence of two molecular species at approximately  $-168$  and  $-23$  °C, the high-temperature form of which dissociates above  $127$  °C, with the oxygen atoms stable up to  $327$  °C.<sup>24–26</sup> At high temperatures ( $\sim 600$  °C) species such as  $O^-$  and  $O^{2-}$  can be expected,<sup>27,28</sup> though the existence of all these forms on titania has not been proven experimentally. Coadsorption of water and oxygen on titania have been studied by experimental and theoretical methods.<sup>29,30</sup> Interaction of ionosorbed oxygen species with adsorbed water is necessary to lead to changes in resistance and can proceed as follows



where



represents an ionosorbed oxygen at a vacancy and  $\text{Ti}^{4+}$  is a five-coordinated titanium species. Reaction 3 has been recently proposed for explaining resistance changes on  $\text{SnO}_2$  upon exposure to water.<sup>31</sup> Reaction 5 involves the displacement of the ionosorbed oxygen as an oxygen atom that can then combine with another O atom to form a molecular species or can diffuse into the bulk or move to another vacancy.<sup>26</sup> Reaction 5 also leads to the initial formation of BH, as observed in the DRIFTS study, and we propose this to be the most likely reaction involved in the resistance change. In both reactions 4 and 5, the effect of water is to modify the oxygen vacancy to a bridging oxygen, effectively annealing the surface.

When the water is turned off, the resistance recovers to the baseline value within  $\sim 15$  min (Figure 1a) and can best be represented by the reverse of reaction 5. The DRIFTS data suggest (Figure 6) that upon removing  $\text{H}_2\text{O}$  from the gas stream the initial effect is the decrease of BH groups, consistent with the chemistry shown in reaction 5.

**Alleviating of the Effects of Adsorbed Water Using a Zeolite Filter.** On the basis of the spectroscopic studies, it is clear that to minimize the impact of water on the resistance of titania water has to be kept away from the semiconductor surface. The influence of water on resistance changes upon reaction of CO with tin oxide has been recently reported.<sup>32</sup> Silicalite membranes have been designed with the intention of separating water from other solvents because the hydrophobic nature of the zeolite favors rejection of water.<sup>33</sup> There have been reports of using zeolite filters for adsorption and altering

reactivity patterns for gases to optimize sensor performance,<sup>13,34</sup> but the data shown in Figures 8 and 9 suggesting that the silicalite filter is effective in rejecting water is the first report for controlling water interference. With hydrated CO, the zeolite filter appears to reject water molecules while admitting CO, even though both gases are introduced simultaneously (Figure 9). The lack of resistance changes also indicates that the filter does not have large pinholes to admit moisture.

Although these data demonstrate that a zeolite filter can be coupled with semiconducting oxides to minimize the effects of moisture, much work remains to be done to optimize the system. For example, the response/recovery times with the filter are significantly longer, on the order of hours, and are impractical. Second, competitive effects of gas permeation in the presence of several gas constituents and the ensuing molecular traffic issues need to be addressed. However, if the membrane concept can be made practical, then discrimination by molecular sieving becomes possible and adds a new tool to promote selectivity of high-temperature semiconducting oxide gas sensors.

## Conclusion

Water is known to cause electrical changes in metal semiconducting oxide systems. The use of high-temperature in situ infrared spectroscopy has made it possible to probe the chemistry of water adsorption on anatase at high temperatures and correlate chemical properties of the surface to changes in electrical resistance of the anatase. It was found that the introduction of water over titania caused a decrease in resistance that stabilized within 3 min and from the in situ infrared studies is correlated with the dissociation of water to bridging hydroxyl groups ( $3660 \text{ cm}^{-1}$ ). Upon removal of the water, the loss in intensity of the bridging hydroxyl groups is also correlated with the recovery in resistance. It is proposed that water dissociation occurs at vacancy sites that chemisorb oxygen with the formation of hydroxyl groups resulting in change in electrical conductivity. The effects of water can be alleviated by placing a hydrophobic zeolite filter in the path of the gas stream. The microporous filter rejects water but lets gases such as CO pass unimpeded through the filter.

**Acknowledgment.** We acknowledge funding from the Department of Energy NETL (DE-FC26-03NT41615) program.

## References and Notes

- (1) Sengupta, G.; Chatterjee, R. N.; Maity, G. C.; Ansari, B. J.; Satyanarayana, C. V. V. *J. Colloid Interface Sci.* **1995**, *170*, 215–219.
- (2) Harkoma-Mattila, A.; Romppainen, P.; Torvela, H.; Leppavuori, S. *J. Eur. Ceram. Soc.* **1990**, *6*, 361–367.
- (3) Ionescu, R.; Vancu, A.; Moise, C.; Tomescu, A. *Sens. Actuators, B* **1999**, *61*, 39–42.
- (4) Heiland, G.; Kohl, D. *Chemical Sensor Technology*; Seiyama, T., Eds.; Elsevier Publishing Company: Toyko, 1988; Vol. 1, Chapter 2, pp 15–38.
- (5) Barsan, N.; Weimar, U. *J. Electroceram.* **2001**, *7*, 143–167.
- (6) Pohle, R.; Fleischer, M.; Meixner, H. *Sens. Actuators, B* **2000**, *68*, 151–156.
- (7) Morterra, C. *J. Chem. Soc., Faraday Trans. 1* **1988**, *84*, 1617–1637.
- (8) Morishige, K.; Kanno, F.; Ogawara, S.; Sasaki, S. *J. Phys. Chem.* **1985**, *89*, 4404–4408.
- (9) Baraton, M. I. *Sens. Actuators, B* **1996**, *31*, 33–38.
- (10) Finnie, K. S.; Cassidy, D. J.; Bartlett, J. R.; Woolfrey, J. L. *Langmuir* **2001**, *17*, 816–820.
- (11) Parkyn, N. D. In *Chemisorption and Catalysis*; Hepple, P., Ed.; Elsevier Publishing: London, 1970; pp 150–171.
- (12) Nakamura, R.; Ueda, K.; Sato, S. *Langmuir* **2001**, *17*, 2298–2300.
- (13) Trimboli, J.; Dutta, P. K. *Sens. Actuators, B* **2004**, *102*, 132–141.
- (14) Savage, N. O.; Akbar, S. A.; Dutta, P. K. *Sens. Actuators, B* **2001**, *72*, 239–248.
- (15) Lovallo, M. C.; Tsapatsis, M. *AIChE J.* **1996**, *42*, 3020–3029.
- (16) Xomeritakis, G.; Nair, S.; Tsapatsis, M. *Microporous Mesoporous Mater.* **2000**, *38*, 61–73.

- (17) Shreedhara-M., R. S.; Blitz, J. P.; Leyden, D. E. *Anal. Chem.* **1986**, *58*, 3167–3172.
- (18) Van Every, K. W.; Griffiths, P. R. *Appl. Spectrosc.* **1991**, *45*, 347–359.
- (19) Simmons, G. W.; Beard, B. C. *J. Phys. Chem.* **1987**, *91*, 1143–1148.
- (20) Henderson, M. A. *Langmuir* **1996**, *12*, 5093–5098.
- (21) Primet, M.; Pichat, P.; Mathieu, M. V. *J. Phys. Chem.* **1971**, *75*, 1216–1220.
- (22) Henrich, V. E.; Cox, P. A. In *The Surface Science of Metal Oxides*; Cambridge University Press: New York, 1994.
- (23) McAleer, J. F.; Moseley, P. T.; Norris, J. O. W.; William, D. F. *J. Chem. Soc.* **1987**, *83*, 1323–1346.
- (24) Lu, G.; Linsebigler, A.; Yates, J. T. *J. Chem. Phys.* **1995**, *102* (11), 4657–4662.
- (25) Henderson, M. A.; Epling, W. S.; Perkins, C. L.; Peden, C. H. F.; Diebold, U. *J. Phys. Chem. B* **1999**, *103*, 5328–5337.
- (26) Epling, W. S.; Peden, C. H. F.; Henderson, M. A.; Diebold, U. *Surf. Sci.* **1998**, *412*, 333–343.
- (27) Iwamoto, M.; Yoda, Y.; Yamazoe, N.; Seiyama, T. *J. Phys. Chem.* **1978**, *82*, 2564–2570.
- (28) Qin, D.; Chang, W.; Chen, Y.; Zhou, J.; Chen, Y.; Gong, M. *J. Catal.* **1993**, *142*, 719–724.
- (29) Hugenschmid, M. B.; Gamble, L.; Campell, C. T. *Surf. Sci.* **1994**, *302*, 329–340.
- (30) Zhang, C.; Lindan, P. J. D. *J. Chem. Phys.* **2004**, *121*, 3811–3815.
- (31) Koziej, D.; Barsan, N.; Weimar, U.; Szuber, J.; Shimanoe, K.; Yamazoe, N. *Chem. Phys. Lett.* **2005**, *410*, 321–323.
- (32) Hahn, S. H.; Barsan, N.; Weimar, U.; Ejakov, S. G.; Visser, J. H.; Soltis, R. E. *Thin Solid Films* **2003**, *436*, 17–24.
- (33) Algieri, C.; Bernardo, P.; Golemme, G.; Barbieri, G.; Drioli, E. *J. Membr. Sci.* **2003**, *222*, 191–190.
- (34) Pijotat, C.; Viricelle, J. P.; Tournier, G.; Montmeat, P. *Thin Solid Films* **2005**, *480* (1), 7–16.